Viscous flow and jump dynamics in molecular supercooled liquids. II. Rotations

Cristiano De Michele[1] and Dino Leporini[1,2,*]

[1]*Dipartimento di Fisica, Università di Pisa, Via Filippo Buonarroti, 2, I-56100 Pisa, Italy*
[2]*Istituto Nazionale di Fisica della Materia, Unità di Pisa, I-56100 Pisa, Italy*
(Received 13 December 1999; published 27 February 2001)

The rotational dynamics of a supercooled model liquid of rigid A-B dumbbells interacting via a Lennard-Jones potential is investigated along one single isobar. The time-temperature superposition principle, one key prediction of mode-coupling theory (MCT), was studied for the orientational correlation functions C_l. In agreement with previous studies we found that the scaling of C_l in a narrow region at long times is better at high-l values. However, on a wider time interval the scaling works fairly better at *low-l* values. Consistently, we observed the remarkable temperature dependence of the rotational correlation time τ_1 as a power law in $T-T_c$ over more than three orders of magnitude and the increasing deviations from that law on increasing l (T_c is the MCT critical temperature). For $0.7 < T < 2$, good agreement with the diffusion model is found. For lower temperatures the agreement becomes poorer, and the results are also only partially accounted for by the jump-rotation model. The angular Van Hove function shows that in this region a meaningful fraction of the sample reorientates by jumps of about 180°. The distribution of the waiting times in the angular sites cuts exponentially at long times. At lower temperatures it decays at short times as $t^{\xi-1}$, with $\xi=0.34\pm0.04$ at $T=0.5$, in analogy with the translational case. The breakdown of the Debye-Stokes-Einstein relation is observed at lower temperatures, where the rotational correlation times diverge more weakly than the viscosity.

I. INTRODUCTION

The relaxation and transport properties of molecular liquids depend on both their translational and rotational motion. Since their mutual interplay cannot be neglected, both dynamical aspects must be jointly considered. If the liquids are supercooled or supercompressed, overwhelming difficulties to molecular rearrangement are expected to enhance the role of the rotational degrees of freedom and, more particularly, the rotational-translational coupling, as noted by experiments [1–5], theory [6–8], and [9–12], numerical studies and discussed in a recent topical meeting [13].

Molecular dynamics (MD) numerical studies provided considerable insight into supercooled liquids in the last years [14]. However, the question of rotational dynamics seems to have been partially overlooked, since most studies dealt with atomic systems where rotational dynamics is missing. Notable exceptions addressed the issue in model systems of disordered dipolar lattice [9], biatomic molecules [10,11], and well studied glass formers, (e.g. CKN [15], o-terphenyl (OTP) [16,17] and methanol [18]). The case of supercooled water was investigated in detail [19]. Studies of plastic crystals and orientational glasses (i.e., no allowed translation) are also known [20,21].

In the previous paper hereafter referred to as I), we presented numerical results on the translational motion of a supercooled molecular model liquid [22]. The present paper seeks to complement I by extending the analysis to rotational degrees of freedom. As in I, one issue is the detection and characterization of jump dynamics. It is found that rotational jumps are more frequent than translational ones in the present system. This makes it easier their study. The occur-rence of jumps poses the question of the coupling of the molecular reorientation with the shear viscous flow. This is the second issue addressed in this paper. Jump dynamics may take place in the absence of any shear flow. Nonetheless, shear motion may favor jumps over energy barriers [23]. The question is of relevance in that the experimental situation is rather controversial. For macroscopic bodies hydrodynamics predicts that the reorientation is strongly coupled to the viscosity η according to the Debye-Stokes-Einstein (DSE) law, $\tau, D_r^{-1} \propto \eta$, where τ and D_r are the rotational correlation time and diffusion coefficient, respectively [24–26]. The DSE law is quite robust. In fact, the coupling of the reorientation to the viscosity is usually found even at a molecular level if the viscosity is smaller of about 1–10 P. At higher values the DSE law overestimates the correlation times of tracers in supercooled liquids according to time-resolved fluorescence [27,28] and electron spin resonance (ESR) studies [5,29,30]. On the other hand, photobleaching [2] and NMR [3] studies found only small deviations from the DSE law even close to T_g. Interestingly, according to ESR studies in the region where tracer reorientation decouples by the viscosity, an ESR study showed that it occurs by jump motion [31,32].

The system under study is a model molecular liquid of rigid dumbbells interacting via the Lennard-Jones potential [10–12]. Atoms A and B of each molecule have mass m and are spaced by d. Atoms on different molecules interact via the Lennard-Jones potential.

$$V_{\alpha\beta}(r) = 4\epsilon_{\alpha\beta}[(\sigma_{\alpha\beta}/r)^{12} - (\sigma_{\alpha\beta}/r)^6], \quad \alpha,\beta \in \{A,B\} \tag{1.1}$$

The potential was cut off and shifted at $r_{cutoff} = 2.5\sigma_{AA}$. Henceforth, reduced units will be used. Lengths are in units of σ_{AA}, energies in units of ϵ_{AA}, and masses in units of m.

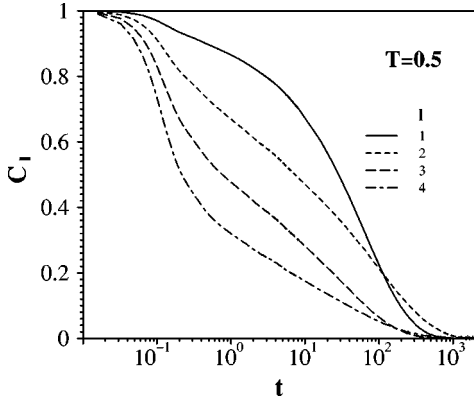*Corresponding author. Email address: dino.leporini@df.unipi.it

FIG. 1. Correlation functions C_1, C_2, C_3, and C_4 at $T=0.5$. C_l decay more at short times by increasing l. The curves with $l=1$ and 3 decay faster at long times than the curves with $l=2$ and 4, respectively, due to the partial head-tail symmetry of the molecules.

The time unit is $(m\sigma_{AA}^2/\epsilon_{AA})^{1/2}$, corresponding to about 2 ps for the argon atom. The pressure P, temperature T, and shear viscosity η are in units of $\epsilon_{AA}/\sigma_{AA}^3$, ϵ_{AA}/k_B, and $\sqrt{m\epsilon_{AA}}/\sigma_{AA}^2$, respectively.

The model parameters in reduced units are $\sigma_{AA}=\sigma_{AB}=1.0$, $\sigma_{BB}=0.95$, $\epsilon_{AA}=\epsilon_{AB}=1.0$, $\epsilon_{BB}=0.95$, $d=0.5$, and $m_A=m_B=m=1.0$. The sample has $N=N_{at}/2=1000$ molecules which are accommodated in a cubic box with periodic boundary conditions. The reader is referred to I for other details. The temperatures we investigated are $T=6$, 5, 3, 2, 1.4, 1.1, 0.85, 0.70, 0.632, 0.588, 0.549, 0.52, and 0.5.

The paper is organized as follows. In Secs. II and III the results are discussed and the conclusions are summarized, respectively.

II. RESULTS AND DISCUSSION

After the outline of the correlation losses of the system, the related correlation times and transport coefficients will be presented. The presence of rotational jumps will be shown, and their waiting time distribution will be discussed. Finally, the decoupling of the relaxation from the viscous flow will be presented.

A. Correlation functions

The rotational correlation functions are defined as

$$C_l(t) = \frac{1}{N} \sum_{i=1}^{N} \langle P_l(\mathbf{u}_i(t) \cdot \mathbf{u}_i(0)) \rangle. \quad (2.1)$$

$\mathbf{u}_i(t)$ is the unit vector parallel to the axis of the molecule i at time t, and $P_l(x)$ the Legendre polynomial of order l. It is worth noting that C_1 and C_2 are accessible to several experimental techniques, e.g., dielectric spectroscopy, NMR, ESR, light scattering, and neutron scattering.

At high temperature and short times, damped oscillations are seen in C_l [10]. They are typical features of free rotators in gaslike systems [20,33]. At lower temperatures, after an initial drop an intermediate regime appears where correlations are lost more slowly. This proves the increased angular trapping. The height of that pseudoplateau decreases with l

(see Fig. 1). This is understood by noting that the oscillatory character of $P_l(\mathbf{u}_i(t) \cdot \mathbf{u}_i(0))$, with respect to the angle between $\mathbf{u}_i(t)$ and $\mathbf{u}_i(0)$, increases with l. Then, by increasing l quickly, small-amplitude angular changes contribute to the decay of C_l. The long-time decay is fairly well described by the stretched exponential $\sim \exp[-(t/\tau)^\beta]$. Upon cooling, the stretching becomes pronounced. At $T=0.5$ we found $\tau=62.9$ and $\beta=0.70$ for $l=1$, $\tau=96.1$ and $\beta=0.60$ for $l=2$, $\tau=32.4$ and $\beta=0.60$ for $l=3$, and $\tau=27.9$ and $\beta=0.47$ for $l=4$. We note that the stretching parameter decreases with increasing l. At such a low temperature, cage effects are important (see I). The subsequent constraints, hampering the reorientation of the trapped molecule, are more suitably detected by high-l C_l correlators. In fact, if l is low, the correlator averages the rotational process at larger angular steps.

Figure 1 shows that a crossing between the pairs C_1 and C_2 and C_3 and C_4 occurs. This is due to the fact that, as will be shown below molecules undergo frequent 180° flips at lower temperatures. Due to the nearly head-tail symmetry, the flips reverse the sign of P_l if l is odd, and then shorten the decay of C_l, whereas no change takes place if l is even.

We investigate in detail one key prediction of mode-coupling theory (MCT), namely that in the long-time region, the so-called α region, the time-temperature superposition principle (TTSP) works better and better upon approaching the critical temperature T_c from above [10]. The TTSP states that changing the temperature simply shifts a correlator on the log-time axis, but does not change its shape. Figure 2 shows the results for $l=1$ and 4. The cases with $l=2$ and 3 are intermediate. Scaling was performed by moving the points where $C_1 = 1/e$ and $C_4 = 0.1$ to coincidence. It must be stressed that the alternative $C_4 = 1/e$ does not collapse the curves. To make the effectiveness of scaling more quantitative, we evaluated the difference between the scaled correlation functions at $T=0.5$ and $T=x$ $\Delta C_{0.5,x}(t/\tau) = C(t/\tau;T=0.5) - C(t/\tau;T=x)$. The results are shown in Fig. 2 for $x=0.520$ and 0.7. These demonstrate effectively that—even if at long times the scaling of C_4 is more effective [10]—on a wider time scale, covering the regions where C_4 is appreciably large, the scaling of C_1 is fairly better. This findings support the conclusion that MCT provides a poor description of the rotational dynamics on finer microscopic scales. This will be further motivated below by the analysis of the rotational correlation times, and is quite consistent with the finding that the so called MCT β correlator fits C_l correlators on shorter and shorter time windows on increasing l [11].

For a linear molecule the angular velocity is $\omega = \mathbf{u} \times \dot{\mathbf{u}}$. A set of correlation functions is defined as

$$\Psi_l(t) = \frac{1}{N} \sum_{i=1}^{N} \langle P_l(\cos \alpha_i(t)) \rangle, \quad l \geq 1. \quad (2.2)$$

$\alpha_i(t)$ is the angle between $\omega_i(t)$ and $\omega_i(0)$. In particular, for $l=1$ one has the usual correlation function of the angular velocity. In Fig. 3, Ψ_1 is drawn for all temperatures investigated. Ψ_1 decays quickly, and increasing T slows down the decay (note the difference from the orientation case). In particular, in the free-rotator limit Ψ_1 is a constant. At lower
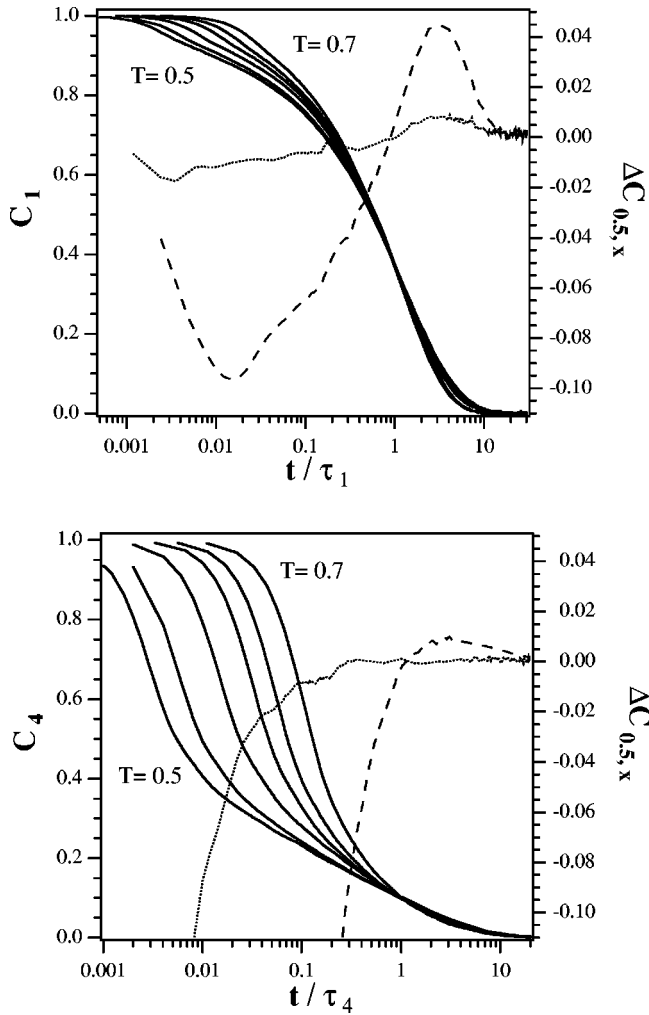
FIG. 2. Scaling analysis of the correlation functions C_1 and C_4 at $T=0.5$, 0.520, 0.549, 0.588, 0.632, and 0.7 (bold lines, left axis). The curves were logarithmically shifted to make the points where $C_1=1/e$ and $C_4=0.1$ coincident. Plots of $\Delta C_{0.5,x}(t/\tau)$ are also shown (right axis) for $x=0.520$ (dotted curves) and $x=0.7$ (dashed curves). See the text for details.

temperatures Ψ_1 shows a negative part at short times, which evidences a change of sign of ω. This must be ascribed to collisions on the rigid cage trapping the molecule. An analogous effect was also noted for the linear velocity correlation function in I. Comparing Ψ_1 and Ψ_2 (see Ref. [10]), shows no significant differences between them at high temperature. At lower temperatures the latter slows down when $\Psi_2 \approx 0.25$, and a long-living tail shows up. This is interpreted by noting that, at lower temperatures, after the ballistic regime the angular velocity is approximately trapped in a circle. As long as the trapping is effective, $\Psi_1(t)=0$, whereas $\Psi_2(t)=0.25$ [20]. When the molecular rearrangement allows an orientation relaxation, the angular velocity tends to be distributed over a sphere, and Ψ_2 vanishes approximately as C_2.

B. Diffusion coefficient and relaxation times

The rotational diffusion coefficient of a linear molecule may be defined by a suitable Green-Kubo formula, in close analogy to the translational counterpart, as [33]
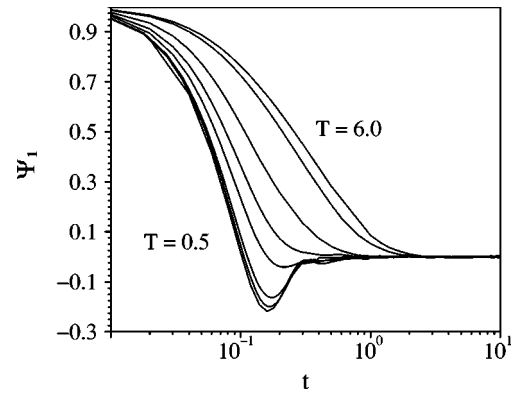

FIG. 3. Correlation functions of the angular velocity Ψ_1, plotted for all the temperatures studied.

$$D_r = \tfrac{1}{2} \int_0^\infty \langle \omega(0)\omega(t) \rangle dt. \qquad (2.3)$$

From a computational point of view, the evaluation of the above integral is delicate, and it is more convenient to evaluate D_r via the Einstein relation [10]

$$D_r = \lim_{t \to \infty} \frac{R_r}{4t}. \qquad (2.4)$$

R_r is the mean squared angular displacement,

$$R_r(t) = \frac{1}{N} \sum_{i=1}^{N} \langle |\phi_i(t+t_0) - \phi_i(t_0)|^2 \rangle, \qquad (2.5)$$

where $\phi_i(t)$ is

$$\phi_i(t) - \phi_i(0) = \Delta \phi_i(t) = \int_0^t \omega_i(t')dt'. \qquad (2.6)$$

$R_r(t)$ is qualitatively similar to the mean squared translational displacement (see I). At short time the motion is ballistic. At intermediate times and lower temperatures a plateau shows up. This signals the increasing trapping of the molecular orientation due to severe constraints on the structure relaxation. At longer times the reorientation is diffusive [Eq. (2.4)]. By comparing $R_r(t)$ with the translational mean square displacement, it is seen that the angular trapping is weaker than the one affecting the center-of-mass motion, since the subdiffusive intermediate regime is less pronounced and extends less on the time scale.

The rotational correlation times are defined as [33]

$$\tau_l = \int_0^\infty C_l(t)dt. \qquad (2.7)$$

Figure 4 presents the T dependence of τ_l, $l=1-4$, and D_r. It is seen that a wide region exists where the above quantities exhibit approximately the same Arrhenius behavior (about $0.7<T<2$). At lower temperatures the apparent activation energy of the rotational correlation times increase. In particular, as noted above, τ_1 becomes shorter than τ_2, and a similar crossover is anticipated between τ_3 and τ_4 at temperatures just below 0.5. Conversely, the rotational diffusion coefficient D_r exhibits the same activated behavior over a region
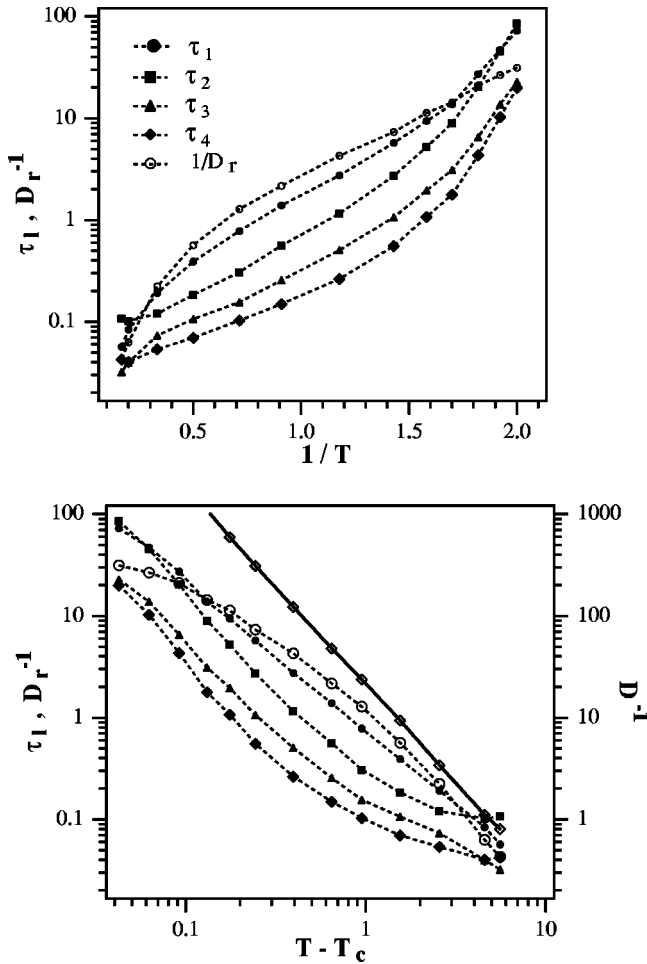
FIG. 4. Arrhenius plot (top) and MCT scaling analysis (bottom) of the rotational correlation times τ_l, $l=1-4$, and the rotational diffusion coefficient D_r. $T_c=0.458$. The dashed lines are guides for the eyes. The translational diffusion constant D is also drawn for comparison (open diamonds). The continuous line is the best fit by using Eq. (2.8), with $\gamma_D=1.93\pm0.02$.

which was also shown to extend below the critical temperature T_c predicted by MCT [10]. The decoupling of D_r with respect to τ_l may be anticipated by noting that the former is related to the area below $\Psi_1(t)$ [Eq. (2.4)], and the latter to the area below $C_l(t)$ [Eq. (2.7)]. At lower temperatures $\Psi_1(t)$ vanishes more quickly, thus probing the fast dynamics of the supercooled liquid, whereas the decay of $C_l(t)$ slows down more and more (see Sec. II A). It has to be noted that even in highly constrained liquids small angular motions, which are unable to relax the orientation, lead to a finite value of D_r in view of Eqs. (2.4) and (2.5) [10]. Such librational motions were detected in a MD study of OTP [16].

Figure 4 also shows the MCT analysis of the T dependence of the correlation time and the rotational diffusion [6,7]. According to MCT, both τ_l and D_r should scale as

$$\tau_l, D_r^{-1} \propto (T-T_c)^{-\gamma}. \tag{2.8}$$

The underlying expectation on scaling (2.8) is that it should work with the same T_c value for any transport coefficient and relaxation time. Conversely, the physical meaning of T_c
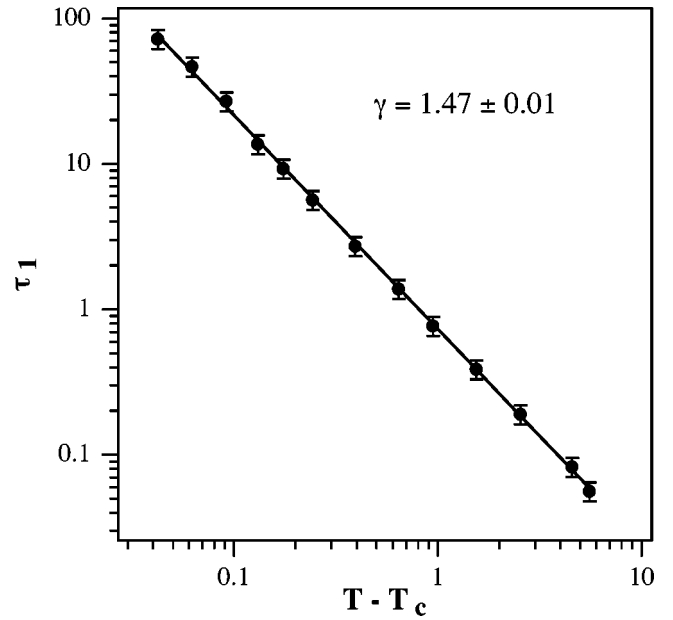

FIG. 5. MCT scaling analysis of τ_1. The superimposed curve is Eq. (2.8), with $\gamma=1.47\pm0.01$ and $T_c=0.458$.

could be weakened. In I it was shown that Eq. (2.8) fits the divergence of the translational diffusion coefficient D over four orders of magnitude with $T_c=0.458\pm0.002$ and $\gamma_D=1.93\pm0.02$ (the data are partially shown in Fig. 4), and that at lower temperatures the primary relaxation time $\tau_\alpha \propto D^{-1}$. Figure 4 shows that scaling (2.8) is also quite effective for τ_1 with $\gamma=1.47\pm0.01$ (also see Fig. 5). However, meaningful deviations are apparent for $l\geq2$ and D_r. The deviations increase as l increases. These findings are nicely consistent with the TTSP analysis presented above, and support the conclusion that mode-coupling theories weaken when dealing with small angular displacements.

To characterize the reorientation process, we studied the quantity $l(l+1)D_r\tau_l$ and the ratio $l(l+1)\tau_l/2\tau_1$. If the molecule rotates by small angular jumps, or if equivalently the waiting time in a single angular site is slightly shorter than the correlation time τ_l, the motion is said to be diffusive, and both quantities are equal to 1 for any l value [25,33]. The results are shown in Fig. 6. Three regions may be broadly defined. For $T>2$ the properties are gaslike, and the rotational correlation times become fairly long. For $0.7<T<2$, $l(l+1)D_r\tau_l$ and $l(l+1)\tau_l/2\tau_1$ do not change appreciably, and are in the range 1–2. For $T<0.7$ the above quantities diverge abruptly. The rapid increase in the deeply supercooled regime demonstrates the failure of the diffusion model, which in fact is expected to work only in liquids with moderate viscosity or if the reorienting molecule is quite large. If the assumption of small angular jumps is released, and proper account is taken of finite jumps with a single average waiting time in each angular site, the so-called jump-rotation model is derived [32]. The main conclusion is that τ_l is roughly independent of l. In fact, for $l=2$ it is found that the quantity $l(l+1)\tau_l/2\tau_1\approx3.5$ at $T=0.5$ (see Fig. 6), and the jump-rotation model predicts a value of about 3. However, at higher l values the comparison be-
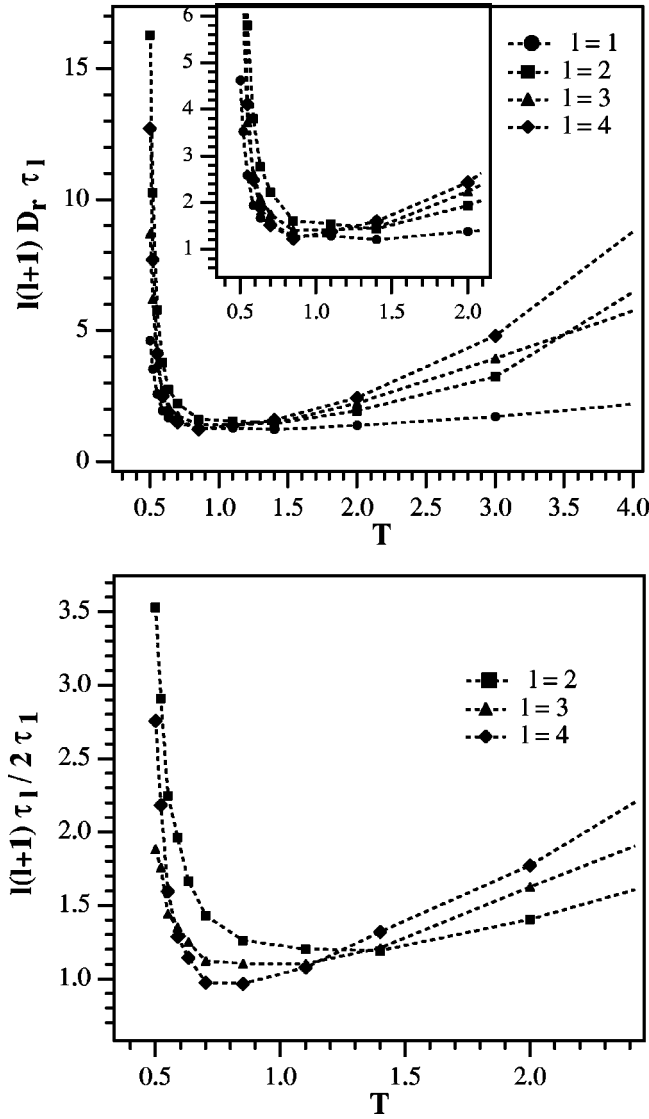
FIG. 6. Temperature dependence of the quantity $l(l+1)D_r\tau_l$ for $l=1$, 2, 3, and 4 (top) and the ratio $l(l+1)\tau_l/2\tau_1$ for $l=2$, 3, and 4 (bottom). If the reorientation is diffusive, both quantities must be equal to 1. If the reorientation is jumplike, $\tau_l \approx \tau_1$.
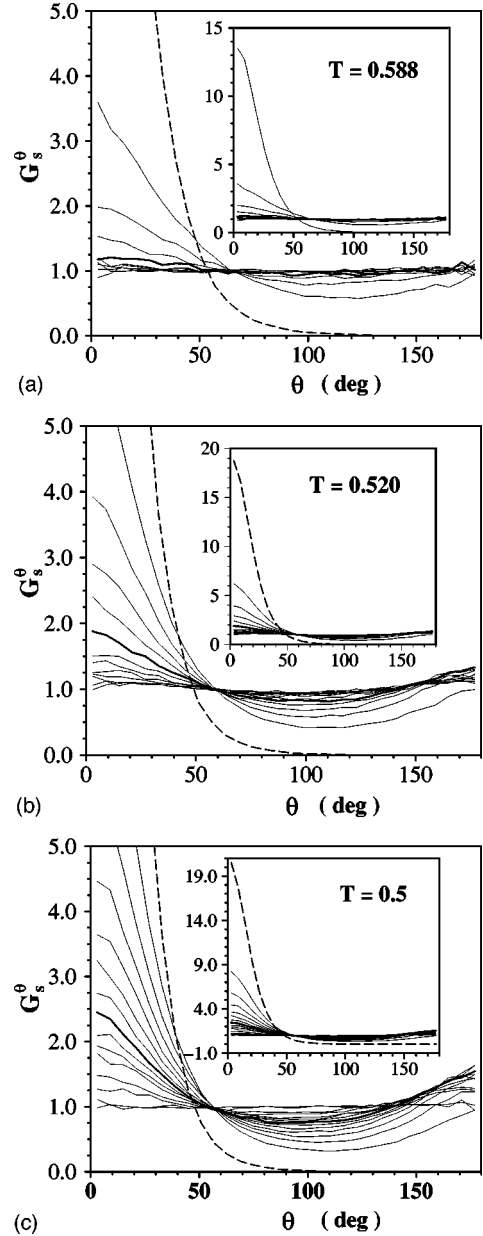

FIG. 7. The angular Van Hove functions at low temperatures. Top: $T=0.588$; bold line: $t=80$. Middle: $T=0.520$; bold line: $t=200$. Bottom: $T=0.5$; bold line: $t=280$. Dashed line: $t=1$. The other continuous lines are plotted at intermediate times with equal spacing.

comes much less favorable. For $l=3$ $l(l+1)\tau_l/2\tau_1 \approx 1.9$ at $T=0.5$, the prediction is about 6. For $l=4$ $l(l+1)\tau_l/2\tau_1 \approx 2.75$, the prediction is about 10. The failure of the usual simple rotational models is not unexpected. Their basic assumptions are rather questionable in supercooled liquids, e.g., the inherent homogeneity of the liquid and the presence of a single time scale both lead to a simple exponential decay of the rotational correlation functions.

C. Jump rotation

The inadequate description provided by the diffusion and the jump model calls for a further characterization of the rotational motion. To this aim we consider the self-part of the angular Van Hove function:

$$G_s^\theta(\theta,t) = \frac{2}{N\sin\theta}\sum_{i=1}^{N}\delta(\theta-\theta_i(t)). \qquad (2.9)$$

$\theta_i(t)$ is the angle between the molecular axis of the ith molecule at the initial time and time t. $1/2G_s^\theta(\theta,t)\sin\theta d\theta$ is the probability that the axis of a molecule is at an angle between θ and $\theta+d\theta$ at time t with respect to the initial orientation. At long times $G_s^\theta(\theta,t) \cong 1$, since all the orientations are equiprobable.

In Fig. 7 the function G_s^θ is plotted for different temperatures and several times. At higher temperatures, as the time goes by, the molecule explores more and more angular sites in a continuous way. Instead, at lower temperatures G_s^θ exhibits a peak at $\theta \approx 180°$ and intermediate times, signaling
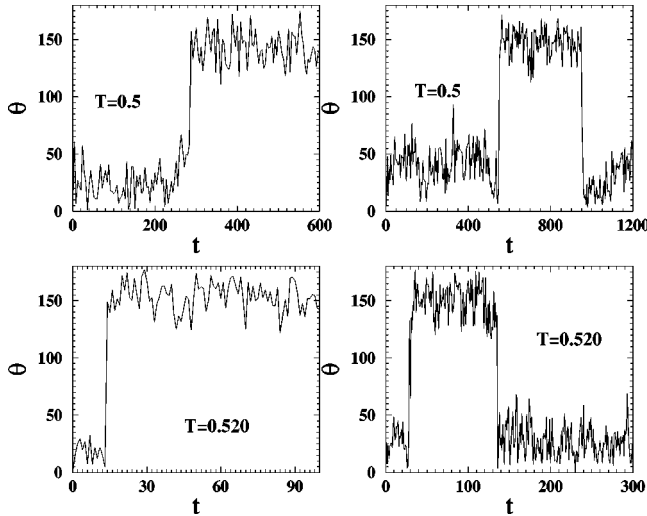
FIG. 8. Selected single-particle orientations evidencing the flips occurring at low temperatures.

that the reorientation has a meaningful probability to occur by jumps.

The indications provided by the Van Hove function concerning the presence of rotational jumps are confirmed by directly inspecting the single-particle trajectories (Fig. 8). Similar findings were also reported in other studies on dumbbells and CKN glass formers [10,15]. With respect to the translational counterparts, it must be pointed out that they are quite a bit faster (see I) and more frequent (about one order of magnitude). The higher number of rotational jumps is also anticipated by noting that, differently from the translational Van Hove function, the rotational function does exhibit explicit signatures of jump motion (see I).

To characterize the jumps, we studied the distribution $\psi_{rot}(t)$ of the waiting time, namely, the residence time in one angular site of the unit vector $\mathbf{u}_i$ parallel to the axis of the ith molecule. A jump of the ith molecule is detected at t_0
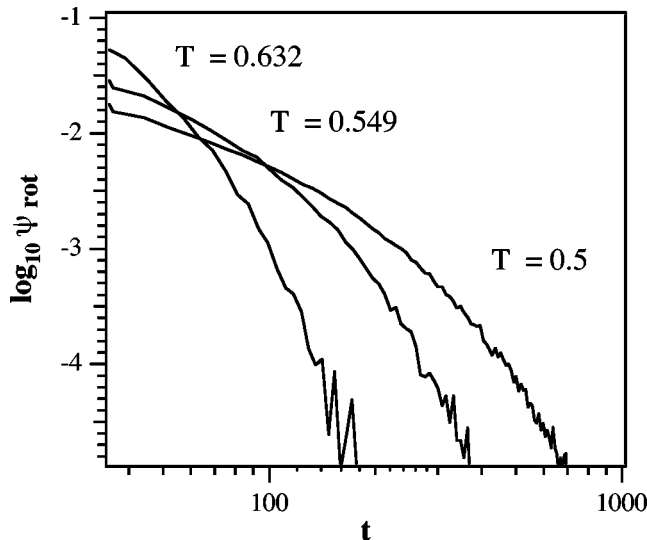

FIG. 9. The rotational waiting-time distribution $\psi_{rot}(t)$ at low temperatures.
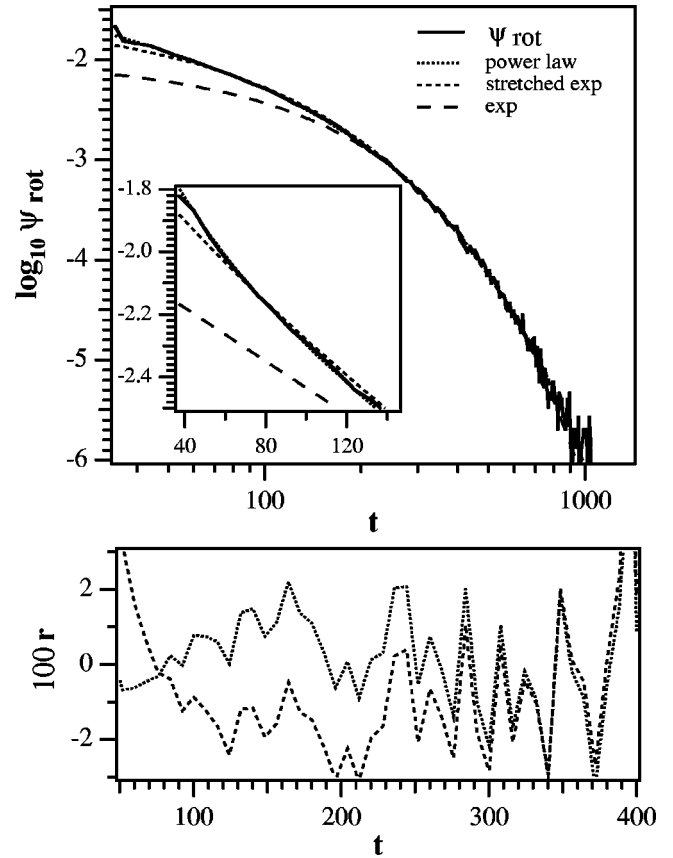

FIG. 10. Analysis of the rotational waiting-time distribution ψ_{rot} at $T=0.5$. Top: comparison of the best fits with the exponential ($\tau=102\pm3$), the stretched exponential (stretching $\beta=0.78\pm0.02$ and $\tau=63\pm4$), and the truncated power law [Eq. (13)] ($\xi=0.34 \pm0.04$ and $\tau=125\pm3$). The inset is a magnification of the short-time region. Note that the fit with the power law is virtually superimposed to ψ_{rot}. Bottom: residuals of the fits in terms of the truncated power law and the stretched exponential.

if the angle between $\mathbf{u}_i(t_0)$ and $\mathbf{u}_i(t_0+\Delta t^*)$ is larger than 100°, with $\Delta t^*=24$. To prevent multiple countings of the same jump, the molecule which jumped at time t is forgotten for a lapse of time Δt^*. To minimize possible contributions due to fast rattling motion, each angular displacement is averaged with the previous and subsequent ones spaced typically by 6–8 time units, depending on the temperature. The jump search procedure was validated by inspecting several single-molecule trajectories. The above definition of rotational jump fits their general features well, i.e. they are rather fast and exhibit no meaningful distribution of either the amplitude or the time needed to complete a jump (see Fig. 8). It is worth noting that in I it was found that the time needed to complete the translational jumps exhibits a distribution. The absence of a similar distribution for the rotational jumps points to the larger freedom of the latter.

Figure 9 shows $\psi_{rot}(t)$ at different temperatures. At $T =0.632$ it is virtually exponential. At lower temperatures deviations become apparent, which are analyzed for $T=0.5$ in Fig. 10. In I it was noted that the translational waiting-time distribution may be fitted nicely by the truncated power law

$$\psi(t)=[\Gamma(\xi)\tau^{\xi}]^{-1}t^{\xi-1}e^{-t/\tau}, \quad 0<\xi\leq1 \qquad (2.10)$$

The best fit provided by Eq. (2.10) is compared to the fits by using the stretched exponential $(\exp[-(t/\tau)^{\beta}])$ and the usual exponential functions in Fig. 10. The better agreement of Eq. (2.10) at short times may be appreciated by looking at the residuals.

The power-law decay of both the translational and rotational waiting-time distributions is an indication that the molecular motion at short times exhibits an intermittent behavior. The issue in the framework of glasses was addressed by several authors [34–38]. In particular, the development of a power-law divergence of the waiting-time distribution at *short times* was predicted by models of trapping in energy landscapes under fairly general assumptions [39].

The exponent ξ of Eq. (2.10) has a simple interpretation. If a dot on the time axis marks a jump, the fractal dimension of the set of dots is ξ. For $\xi<1$, it follows that $\psi(t)\propto t^{\xi-1}$ at short times [34,40], in agreement with our results. If $\xi=1$, the distribution of dots is uniform, and $\psi(t)$ recovers an exponential form. This is expected beyond a time scale τ, and the exponential decay of $\psi_{rot}(t)$ at long times signals the crossover to the usual Poisson regime. It must be noted that the translational waiting-time distribution at the lowest temperature ($T=0.5$) shows a weak tendency to vanish faster than Eq. (2.10) at long times. A similar feature is not observed in $\psi_{rot}(t)$.

D. Breakdown of the Debye-Stokes-Einstein law

For large Brownian particles the reorientation in a liquid occurs via a series of small angular steps, i.e., it is diffusive. Hydrodynamics predicts that the diffusion manifests a strong coupling to the viscosity η which is accounted for by the Debye-Stokes-Einstein law. For biaxial ellipsoids, it takes the form [25]

$$D_{i}=\frac{kT}{\mu_{i}\eta}, \quad i=x,y,z. \qquad (2.11)$$

$D_{x,y,z}$ are the principal values of the diffusion tensor, and k is the Boltzmann constant. The coefficients μ_{i} depend on the geometry and the boundary conditions (BC's). For a sphere with stick BC's $\mu_{x,y,z}=6v$, v being the volume of the sphere. For an uniaxial ellipsoid one considers $D_{\parallel}=D_{z}$ and $D_{\perp}=D_{x}=D_{y}$. The case of stick BC's can be worked analytically [24,25]. For slip BC's numerical results for $D_{\perp}$ are known [26] (note that in this case the fluid does not exert torques parallel to the symmetry axis). Equation (2.11) is sometimes rewritten in an alternative form in terms of proper rotational correlation times, e.g., for uniaxial molecules the equality $\tau_{l}=1/l(l+1)D_{\perp}$ holds. The new form is more suitable for a comparison with the experiments, since experiments do not usually provide direct access to the rotational diffusion coefficients. However, this form assumes that the rotational diffusion model holds.

Irrespective of the heavy hydrodynamic assumptions, the DSE law works nicely even at a molecular level if the viscosity is not high ($\eta<1$ P). Deviations are observed at higher viscosities for tracers in supercooled liquids by time-
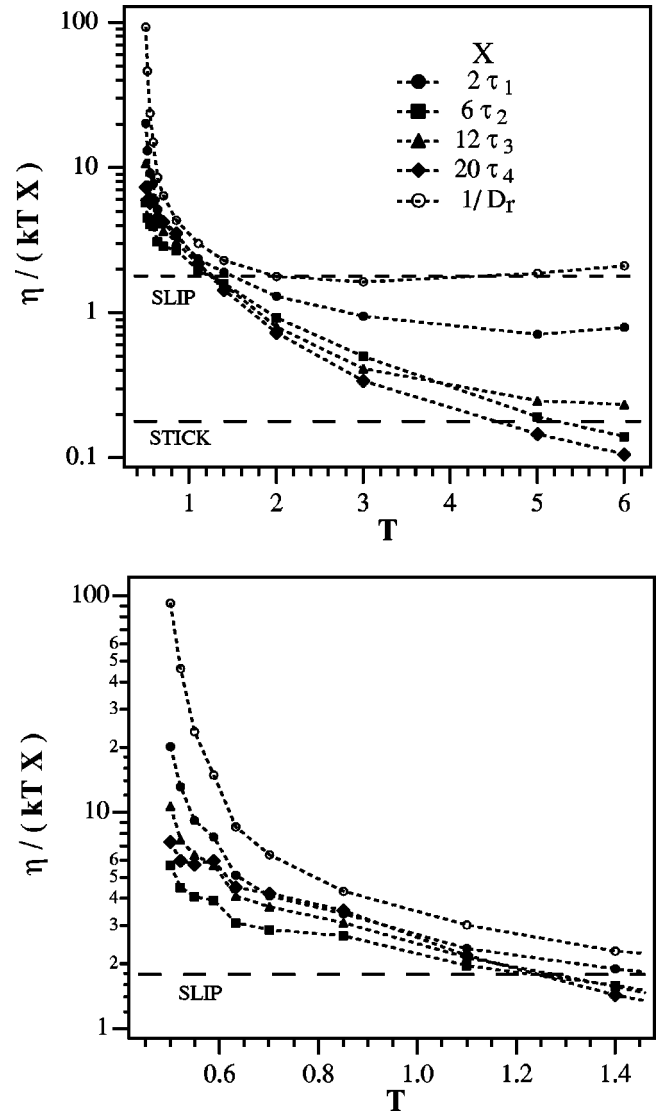

FIG. 11. Plots of the quantity η/XkT with $X=D_{r}^{-1},l(l+1)\tau_{l}$ over the overall temperature range (top) and in the supercooled regime (bottom). The superimposed dashed lines are the DSE expectations for stick and slip boundary conditions for a prolate ellipsoid with semiaxes 3/2 and 1/2. Note that at $T=1.4$, η/XkT depends little on X, signaling diffusive behavior.

resolved fluorescence [27,28] and electron spin resonance studies [5,29,30]. On the other hand, photobleaching [2] and NMR [3] studies found only small deviations from the DSE law even close to T_{g}. In all the cases known, the DSE law is found to overestimate the rotational correlation times, since on cooling their increase is less than the one exhibited by the viscosity. In this decoupling region ESR evidenced that the tracer under investigation rotates by jump motion [31].

Shear motion facilitates molecular jumps over energy barriers [23]. On the other hand, "guest" molecules may jump in frozen hosts in the absence of viscous flow. Since a meaningful fraction of the molecule in the system reorientates by finite angular steps with intermittent behavior, not quite expected in a liquid, it is of interest to investigate to what extent the reorientation is coupled to the viscous shear flow.

The results are shown in Fig. 11 by plotting the quantity η/XkT with $X=D_r^{-1}, l(l+1)\tau_l$, where $l=1-4$. According to the DSE law it should be constant. The viscosity data were taken from I. At high temperatures the quantity approaches the value expected for stick BC's. For $T>5$ a tendency of η/XkT for $X=D_r,\tau_1$ to increase is noted. However, at such temperatures the system manifests gaslike features. On cooling, η/XkT increases. For intermediate temperatures the liquid properties are well developed, the system is diffusive [$l(l+1)\tau_lD_r\approx1$; see Fig. 6], and η/XkT has a value close to the DSE expectation with slip BC's. Notably, $D_r\eta/kT$, i.e., the key quantity to assess Eq. (2.11) remains close to this value in the wide interval $2<T<6$. At lower temperatures, η/XkT diverges. Stronger deviations are exhibited by D_r and τ_1, and weaker ones by τ_2. τ_3 and τ_4 track the behavior of τ_1 and τ_4, respectively, the pair $\tau_{1,3}$ being affected by the jump motion much more than the pair $\tau_{2,4}$ (see above). η increases of a factor of about 400 between $T=1.4$ and 0.5. The corresponding changes of $D_r\eta/kT$, η/τ_1kT and η/τ_2kT are 41, 11, and 3.6, respectively. The discussion supports the conclusion that the correlators are affected by rotational jumps, e.g. $C_{1,3}(t)$, yielding correlation times slightly more decoupled by the viscosity.

If one compares the changes of η/τ_2kT to the ones drawn by ESR and fluorescence experiments in the region $T/T_c\approx1.1-1.5$, a broad agreement is found [27,5]. These experiments found even larger values of η/τ_2kT on approaching T_g. Conversely, photobleaching studies detected changes of less than an order of magnitude by changing η over about 12 orders of magnitude, these changes are much smaller than the present ones [2].

Inspection of Fig. 11 suggests a way to reconcile, at least partially, ESR [5], photobleaching [2] and NMR [3] studies on the glass former o-terphenyl (OTP). Both photobleaching and NMR measure τ_2 in a direct way. In the glass transition region the ESR line shape depends in principle on several τ_l's, and a model is needed to relate them to each other and lead to τ_2 [31]. The model is adjusted by fitting the theoretical prediction with the highly structured ESR line shape. Figure 11 shows that the decoupling, as expressed by η/τ_lkT, increases with l. Since the weight of τ_l to set the ESR line shape is roughly comparable, one may anticipate that τ_2^{ESR} may be underestimated at some degree *around* the glass transition. On the other hand, it must be pointed out that rotational decoupling is observed up to $1.4T_g$ in OTP, where ESR yields τ_2 in a model-independent way [5]. Furthermore, the decoupling is also evidenced by fluorescence experiments, which provide τ_2 in a model-independent way [27].

III. CONCLUSIONS

The present paper investigated the rotational dynamics of a supercooled molecular system. The study addressed several general features, and focused on a characterization of the jump dynamics and the degree of coupling with the viscosity.

The ensemble consists of rigid A-B dumbbells interacting via a Lennard-Jones potential. All the properties were studied along the isobar $P=1.5$. The time orientation correlation functions $C_l(t)$ exhibit gaslike features at high temperatures. In the supercooled regime, after a first initial decay, a quasiplateau signals the trapping of the molecule due to the increased difficulty of the surroundings to rearrange themselves. The plateau height decreases by increasing the l rank due to the larger sensitivity to small-angle librations. The long-time decay of $C_l(t)$ is fairly well described by a stretched exponential. The stretching decreases at low-l values. In fact, $C_l(t)$ correlators with low-l values are sensitive to large angular displacements, and are then affected by an effective time-averaged rotational process.

The influence on the decay of C_l (and then on τ_l) of the partial head-tail symmetry of the dumbbells was noted. This leads to crossings between C_1 and C_2 and C_3 and C_4.

The time-temperature superposition (TTSP) shows up on approaching the critical temperature T_c from above. On increasing l, TTSP scaling of C_l becomes rather effective in a narrow region at long times [10]. However, on wider time scales the scaling improves by *decreasing l*.

Remarkably, the temperature dependence of τ_1 is well described by a power law in $T-T_c$ over more than three orders of magnitude, with an exponent $\gamma=1.47\pm0.01$. This parallels the analogous results for the translation diffusion coefficient and the primary relaxation time τ_α in I. On the other hand, deviations of τ_l due to that power law increase with l. This is quite consistent with the TTSP study. Such findings are ascribed to the difficulties which mode-coupling theories meet at short length scales and small angular displacements [41,42].

For $0.7<T<2$ the quantities $l(l+1)D_r\tau_l$ and $l(l+1)\tau_l/2\tau_1$ do not change appreciably, and are in good agreement with the diffusion model, which predicts that both of them are equal to 1 independently of the temperature. For $T<0.7$ the above quantities increase abruptly. The increase of the quantity $l(l+1)\tau_l/2\tau_1$ is reasonably accounted for by the jump-rotation model for $l=2$ [32]. For higher l values the agreement becomes quite poor. As τ_1 and τ_2 were measured in most experiments [2–5,28,43], this finding may account for the attention that the jump model has attracted during the last years [31,44,45].

The analysis of the angular Van Hove function shows that in this region a meaningful fraction of the sample reorientates by jumps of about 180°. The flips are rather quick, and exhibit no meaningful distribution of both the amplitude and the time needed to complete a jump. Conversely, it was noted in I that translational jumps require different times to occur. The absence of a similar effect for the reorientations indicates a larger angular freedom. This is also apparent by the larger number of rotational jumps which are detected with respect to translational ones. It is worth noting that the ease of jumping does not lead to trivial relaxation properties, as signaled by the stretched decay of $C_{1,2,3,4}$.

We characterized the distribution ψ_{rot} of the waiting times in angular sites. This vanishes exponentially at long times, whereas at lower temperatures it decays at short times as $t^{\xi-1}$ with $\xi=0.34\pm0.04$ at $T=0.5$. Interestingly, the translational waiting-time distribution exhibits the same behavior (see I). The exponent for the translational case is ξ

=0.49. We ascribe the power law to the intermittent features of the motion in glassy systems [34–37]. In particular, a power-law divergence of the waiting-time distribution at *short times* is predicted by models of trapping in energy landscapes under fairly general assumptions [39].

The intermittent jump reorientation is somewhat different from motion in a liquid. There, a decoupling from the viscous flow and the subsequent breakdown of the Debye-Stokes-Einstein law is anticipated. Our study confirms this breakdown, and shows that the quantity η/XkT, with $X = D_r^{-1}, l(l+1)\tau_l$, and $l=1-4$ diverges below $T=1$. In particular, the correlators affected by rotational jumps, e.g., $C_{1,3}(t)$, yield correlation times that are slightly more decoupled by the viscosity. A rather similar decoupling was found in I for the product $D\eta$, D being the translational diffusion coefficient.

The decoupling of the molecular reorientation by the viscosity could be also anticipated by the observed ease with which rotational jumps are performed. The reduced tendency to freeze the rotational degrees of freedom was pointed out by MD [9] and theoretical [6] studies. The former investigated residual rotational relaxation in a random lattice with *quenched translations*, and the latter predicted a hierarchy for the glassy freezing; i.e., the rotational dynamics can never freeze *before* the translational dynamics. The decou-pling of the rotational motion of guest molecules from the viscous flow was seen experimentally by time-resolved fluorescence [27,28] and electron spin resonance [5,29,30], while photobleaching and NMR studies reported small deviations from the DSE law even close to T_g [2,3]. It is worth noting that the decoupling of the translational diffusion from the viscosity, and related phenomena like the so-called rotation-translation paradox, have been ascribed to a spatial distribution of mobility and relaxation properties, so called dynamical heterogeneities [2,4,46–50]. Their role will be addressed in a forthcoming study.

Note Added: The related problem of reorientation relaxation of a linear probe molecule in a simple liquid in the framework of mode-coupling theory of a glass transition was discussed in Ref. [51].

[1] For a short review, see M.D. Ediger, C.A. Angell, and S.R. Nagel, J. Phys. Chem. **100**, 13 200 (1996).

[2] M.T. Cicerone, F.R. Blackburn, and M.D. Ediger, J. Chem. Phys. **102**, 471 (1995); M.T. Cicerone and M.D. Ediger, *ibid.* **104**, 7210 (1996).

[3] F. Fujara, B. Geil, H. Sillescu, and G. Fleischer, Z. Phys. B **88**, 195 (1992); I. Chang, F. Fujara, B. Geil, G. Heuberger, T. Mangel, and H. Sillescu, J. Non-Cryst. Solids **172-174**, 248 (1994).

[4] D.B. Hall, A. Dhinojwala, and J.M. Torkelson, Phys. Rev. Lett. **79**, 103 (1997).

[5] L. Andreozzi, A. Di Schino, M. Giordano, and D. Leporini, Europhys. Lett. **38**, 669 (1997).

[6] R. Schilling and T. Scheidsteger, Phys. Rev. E **56**, 2932 (1997).

[7] T. Franosch, M. Fuchs, W. Götze, M.R. Mayr, and A.P. Singh, Phys. Rev. E **56**, 5659 (1997); W. Götze, J. Phys.: Condens. Matter **11**, A1 (1999); H.Z. Cummins, *ibid.* **11**, A95 (1999).

[8] G. Diezemann, H. Sillescu, G. Hinze, and R. Böhmer, Phys. Rev. E **57**, 4398 (1998).

[9] S. Ravichandran and B. Bagchi, Phys. Rev. Lett. **76**, 644 (1996).

[10] S. Kämmerer, W. Kob, and R. Schilling, Phys. Rev. E **56**, 5450 (1997).

[11] S. Kämmerer, W. Kob, and R. Schilling, Phys. Rev. E **58**, 2141 (1998).

[12] S. Kämmerer, W. Kob, and R. Schilling, Phys. Rev. E **58**, 2131 (1998).

[13] *Proceedings of the Second Workshop on Non-Equilibrium Phenomena in Supercooled Fluids, Glasses and Amorphous Materials*, edited by M. Giordano, D. Leporini, and M.P. Tosi [J. Phys.: Condens. Matter **11**, (1999)].

[14] For a review, see W. Kob, J. Phys.: Condens. Matter **11**, R85 (1999).

[15] G.F. Signorini and J.-L. Barrat, J. Chem. Phys. **92**, 1294 (1990).

[16] L.J. Lewis and G. Wahnström, J. Non-Cryst. Solids **172-174**, 69 (1994); Phys. Rev. E **50**, 3865 (1994).

[17] S.R. Kudchakar and J.M. Wiest, J. Chem. Phys. **103**, 8566 (1995).

[18] P. Sindzingre and M.L. Klein, J. Chem. Phys. **96**, 4681 (1992).

[19] P. Gallo, F. Sciortino, P. Tartaglia, and S.-H. Chen, Phys. Rev. Lett. **76**, 2730 (1996); S.-H. Chen, P. Gallo, F. Sciortino, and P. Tartaglia, Phys. Rev. E **56**, 4231 (1997); F. Sciortino, L. Fabbian, S.-H. Chen, and P. Tartaglia, *ibid.* **56**, 5397 (1997).

[20] C. Renner, H. Löwen, and J.L. Barrat, Phys. Rev. E **52**, 5091 (1995).

[21] S.J. Lee and B. Kim, Phys. Rev. E **60**, 1503 (1999).

[22] C. De Michele and D. Leporini, preceding paper, Phys. Rev. E **63**, 036701 (2001).

[23] S. Glasstone, K.J. Laidler, and H. Eyring, *The Theory of Rate Processes* (McGraw-Hill, New York, 1941).

[24] H. Lamb, *Hydrodynamics*, 6th ed. (Cambridge University Press, Cambridge, England, 1932).

[25] L.D. Favro, Phys. Rev. **119**, 53 (1960).

[26] C.-M. Hu and R. Zwanzig, J. Chem. Phys. **60**, 4354 (1974).

[27] J.Y. Ye, T. Hattori, H. Nakatsuka, Y. Maruyama, and M. Ishikawa, Phys. Rev. B **56**, 5286 (1997).

[28] J.C. Hooker and J.M. Torkelson, Macromolecules **28**, 7683 (1995).

[29] L. Andreozzi, M. Giordano, and D. Leporini, J. Non-Cryst. Solids **235-237**, 219 (1998).

[30] M. Faetti, M. Giordano, L. Pardi, and D. Leporini, Macromolecules **32**, 1876 (1999).

[31] L. Andreozzi, F. Cianflone, C. Donati, and D. Leporini, J. Phys.: Condens. Matter **8**, 3795 (1996).

[32] E.N. Ivanov, Zh. Éksp. Teor. Fiz. **45**, 1509 (1963) [Sov. Phys. JETP **18**, 1041 (1964)]; K.A. Valiev and E.N. Ivanov, Usp. Fiz. Nauk **109**, 31 (1973) [Sov. Phys. Usp. **16**, 1 (1973)].

[33] J.-P. Hansen and I.R. McDonald, *Theory of Simple Liquids*, 2nd ed. (Academic Press, London, 1986).

[34] L. Sjögren, Z. Phys. B **74**, 353 (1989).

[35] J.F. Douglas and J.B. Hubbard, Macromolecules **24**, 3163 (1991); J.F. Douglas, Comput. Mater. Sci. **4**, 292 (1995).

[36] T. Odagaki, Phys. Rev. Lett. **75**, 3701 (1995).

[37] P. Allegrini, J.F. Douglas, and S.H. Glotzer, Phys. Rev. E **60**, 5714 (1999).

[38] T. Muranaka and Y. Hiwatari, J. Phys. Soc. Jpn. **67**, 1982 (1998).

[39] J.P. Bouchaud, J. Phys. I **2**, 1705 (1992); C. Monthus and J.P. Bouchaud, J. Phys. A **29**, 3847 (1996).

[40] R. Hilfer and L. Anton, Phys. Rev. E **51**, R848 (1995).

[41] T. Franosch and W. Götze, Phys. Rev. E **57**, 5833 (1998).

[42] U. Balucani and M. Zoppi, *Dynamics of the Liquid State* (Clarendon, Oxford, 1994).

[43] N.G. McCrum, B.E. Read, and G. Williams *Anelastic and Dielectric Effects in Polymeric Solids* (Wiley, New York, 1967).

[44] G. Williams and P.J. Hains, J. Chem. Soc., Faraday Trans. **6**, 14 (1972).

[45] M.S. Beevers, J. Crossley, D.C. Garrington, and G. Williams, J. Chem. Soc., Faraday Trans. 2 **73**, 458 (1977).

[46] J.A. Hodgdon and F.H. Stillinger, Phys. Rev. E **48**, 207 (1993); F.H. Stillinger and J.A. Hodgdon, *ibid.* **50**, 2064 (1994).

[47] C.Z.-W. Liu and I. Oppenheim, Phys. Rev. E **53**, 799 (1996).

[48] J.F. Douglas and D. Leporini, J. Non-Cryst. Solids **235-237**, 137 (1998).

[49] H. Sillescu, J. Non-Cryst. Solids **243**, 81 (1999).

[50] W. Kob, C. Donati, S.J. Plimpton, P.H. Poole, and S.C. Glotzer, Phys. Rev. Lett. **79**, 2827 (1997); C. Donati, J.F. Douglas, W. Kob, S.J. Plimpton, P.H. Poole, and S.C. Glotzer, *ibid.* **80**, 2338 (1998).

[51] W. Götze, A.P. Singh, and Th. Voigtmann, Phys. Rev. E **61**, 6934 (2000).